

---

---

**Prediction of Device Temperatures  
with Depth-Averaged Models of the Flow Field  
over Printed Circuit Boards**

**Gerald W. Recktenwald**  
Department of Mechanical Engineering  
Portland State University  
Portland, Oregon

**ABSTRACT**

Convective heat transfer from electronic devices mounted on a printed circuit board is simulated with an efficient Computational Fluid Dynamics (CFD) model. The computer time necessary to calculate a solution to the flow field is greatly reduced by solving the depth-averaged (DA) flow equations for the fluid flowing above the devices. The DA flow field is then coupled to the full, three-dimensional energy equation in the fluid and in the solid materials comprising the circuit board and the electronic devices. Because the temperature is determined by solving the conjugate problem, no heat transfer coefficient needs to be specified on the outer surface of the devices. This paper provides an overview of the theory behind the depth-averaged and three-dimensional energy equation models. Incorporation of the essentially two-dimensional depth-averaged flow fields in the three-dimensional energy equation is described. The combination of the DA flow field and the three-dimensional energy equation does not yield the same level of detail as a conventional three-dimensional CFD code. The advantage of this approach, however, is that it makes significantly lower demands on the computational hardware and it obtains useful solutions in much less time than conventional CFD codes.

**Introduction**

Technological advances in semiconductor electronics have produced computer components with increasing sophistication and increasing numbers of transistors per component. An unwanted consequence of higher circuit density is an increase in the power dissipation rate per unit volume

for the individual components and for the computer cabinet in which they are housed. As a result thermal management of electronic components and electronic enclosures has become an integral part of electronic equipment design.

The topological complexity of electronic equipment makes it difficult to apply the results of classic theoretical and experimental studies to the details of thermal problems in electronic packaging. A single board is placed in a cabinet that forms complex flow passages, which can be changed as optional cards are added or removed. Circuit boards are assembled from small devices having varying sizes and shapes. Though there is a trend toward fewer, larger packages, circuit boards still have a geometric complexity far beyond that found in the classical problems of convective heat transfer. To address this gap in information many studies have been performed for the geometry and flow regimes found in electronic equipment.

Moffat and Ortega (1988) survey a broad range of experimental data applicable to circuit board analysis. Given an adiabatic heat transfer coefficient and the thermal wake function one can estimate the average temperature of an electronic device with relatively simple calculations. The utility of this approach has been demonstrated by comparison with detailed computer modeling (Anderson, 1994).

The intense competition and short product design cycles in the computer industry require that packaging engineers find design solutions quickly. This pressure has resulted in the development and use of computer-based design tools. Thermal network methods have been used to create models of varying detail and complexity. This technique can be used to simulate the internal details of a single component, or an entire computer cabinet. Ellison (1989) describes net-

work and analytical procedures for thermal as well as flow modeling.

Finite-element, finite-difference and other types of discrete models are used with increasing regularity. Multidimensional heat conduction models have been used to study the temperature distribution inside of components and in the circuit board (Hardisty & Abboud, 1990; De Mey & Van Schoor, 1988; Chen & Chang, 1987). Conduction-only models require knowledge of the heat transfer coefficient between the component and the coolant. Given the internal complexity of integrated circuit packages, these heat conduction models will continue to be very important to designers. The shortage of data on local heat transfer coefficients for the complex geometries found in electronic cooling applications, however, is the primary weakness of this approach.

Commercial packages have emerged that are dedicated to thermal analysis of printed circuit boards and enclosures for electronic equipment. General purpose computational fluid dynamics (CFD) packages are capable of modeling the full spectrum of problems—from individual electronic devices, to full computer cabinets—faced by a packaging engineer. The drawback to using these codes is the cost in computer hardware necessary to use the software, and the time necessary to achieve a complete analysis. Neither the hardware cost or the time investment prevents the use of these techniques, yet both are an obstacle to routine use.

Several numerical studies with two-dimensional CFD codes have been published. Early models involved ducts with flush mounted heaters (Incropera *et al.*, 1986) and ducts with two-dimensional ribs transverse to the main flow (Davalath & Bayazitoglu, 1987; Zebib & Wo, 1989; Agonafer & Moffatt, 1990).

Detailed three-dimensional models are feasible, but the time to achieve the numerical solution on a workstation class computer is longer than many packaging engineers are willing to wait. Anderson (1993) used a commercial CFD code to perform a 3D simulation of a single column of heated blocks. Each run took 16 hours on an IBM 540 scientific workstation.

Waiting several hours for the completion of one simulation is a major drawback to using fully three-dimensional CFD codes. In response we have developed a board-level modeling technique using an adaptation of CFD. A numerical solution to two-dimensional flow equations is coupled with a numerical solution to the three-dimensional energy equation. The result is the temperature distribution in the electronic components and in the fluid. This new analysis method lies on the spectrum between conduction solvers requiring heat transfer coefficients as inputs, and full CFD simulations which require extensive computing resources.

The approach described in this paper requires the introduction of mathematical simplifications and semi-empirical

models. The two-dimensional flow equations are obtained by analytically integrating the three-dimensional continuity and momentum equations across the fluid layer above the electronic devices. The result are the so-called depth-averaged (DA) flow equations. Since the devices protrude from the circuit board, the fluid layer has a variable depth. The shear stresses on the top and bottom of the fluid layer are included in the depth-averaged momentum equations via correlations of shear stress for fully-developed duct flow. Variations in depth of the fluid layer result in pressure and wall shear stress variations in the DA momentum equations. The topology of the circuit board, therefore, influences the flow.

The DA flow field is used in the solution of the three-dimensional energy equation in the fluid layer and in the electronic devices. By solving the conjugate heat transfer problem the need to specify a heat transfer coefficient is eliminated. The DA flow field, however, lacks information about the vertical velocity component, and the vertical variations of the velocity components parallel to the plane of the circuit board. This information is provided by models derived from fully-developed flow.

The DA flow and three-dimensional energy equation models are embodied in separate computer codes that exchange information. The overall problem specification process is managed by a preprocessor that serves as a user interface to the two analysis codes. The result of these efforts is a computer package called the Printed Circuit Board Convection Analysis Tools, or PCBCAT. In a companion paper (Recktenwald, 1995) the PCBCAT are described from the perspective of someone using the tools to model a circuit board.

The goals of this paper are to (1) review the basic DA model equations for momentum and mass conservation, (2) present models for shear stress used in the DA model, (3) explain how the two-dimensional, DA flow field is used in the solution to the three-dimensional energy equation model, and (4) present the eddy viscosity turbulence model used in the solution to the three-dimensional energy equation.

The following section summarizes the numerical modeling and solution algorithms embodied in the PCBCAT codes. First the DA continuity and momentum equations are presented and their solution with the standard pressure-correction based solvers is outlined. Then the three-dimensional energy equation is discussed. The essential step of transforming the DA flow field into a suitable three-dimensional flow field for use in the energy equation is shown in detail.

### Depth-Averaged Model

The depth-averaged equations are derived from the three-dimensional Navier-Stokes equations for the flow of a New-

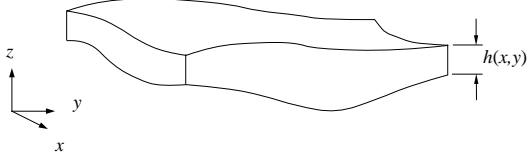


Figure 1: A thin layer of fluid suitable for depth-averaging.

tonian fluid, see e.g, Currie (1993).

$$\frac{\partial \rho}{\partial t} + \frac{\partial}{\partial x_i} (\rho v_i) = 0 \quad (1)$$

$$\frac{\partial}{\partial t} (\rho v_j) + \frac{\partial}{\partial x_i} (\rho v_i v_j) = -\frac{\partial p}{\partial x_j} + \frac{\partial \tau_{j,i}}{\partial x_i} \quad (2)$$

The unsteady terms in these equations must be included to properly affect the transformation to the DA form. The final computer implementation involves solution of only the steady equations. To reduce the three-dimensional flow equations to two-dimensional DA equations, assume that the domain of interest is a relatively thin layer of fluid as represented by the sketch in Figure 1. At any position in the  $x$ - $y$  plane let  $b(x, y)$  be the  $z$  location of the bottom of the fluid layer and  $\ell(x, y)$  be the  $z$  location of the lid of the fluid layer. The layer thickness,  $h$ , is defined by

$$h(x, y) \equiv \ell(x, y) - b(x, y) \quad (3)$$

The depth-averaged equations are obtained by integrating over the narrow gap in the  $z$  direction. The result is (with  $i = 1, 2$  only)

$$\frac{\partial}{\partial t} (\rho h) + \frac{\partial}{\partial x_i} (\rho \bar{v}_i h) = 0 \quad (4)$$

$$\begin{aligned} \frac{\partial}{\partial t} (\rho \bar{v}_j h) + \frac{\partial}{\partial x_i} (\rho \bar{v}_i \bar{v}_j) = \\ -\frac{\partial \bar{p}}{\partial x_j} + \frac{\partial}{\partial x_i} (h \bar{\tau}_{j,i}) + (\tau_{z,j})_\ell - (\tau_{z,j})_b \end{aligned} \quad (5)$$

where the DA velocities and shear stresses are

$$\bar{v}_j \equiv \frac{1}{h} \int_b^\ell v_j dz \quad \bar{\tau}_{j,i} \equiv \frac{1}{h} \int_b^\ell \tau_{j,i} dz \quad (6)$$

### Shear Stress on Bottom and Lid Surfaces

Depth-averaging of the conservation equations removes the  $z$ -direction variations of the dependent variables and it introduces  $z$ -direction flux terms on the bottom and lid surfaces of the domain. In the momentum equations these flux terms are shear stresses. At this point we must directly introduce a model to relate the bottom and lid shear stresses to the DA velocities.

The flow field over and around the electronic components on a PCB is complex and three-dimensional. There are recirculation zones upstream and downstream from the components. The DA model cannot resolve recirculation regions with vertical ( $z$ -direction) velocity components. Without solving the three-dimensional momentum equations there is no way to incorporate vertical velocity components. The choice, then, is how best to represent the bottom and lid shear stresses in a way that is computationally economical while retaining the basic behavior of the flow. The only solution we have found is to use the fully-developed velocity profiles for laminar and turbulent flow.

The DA flow equations implicitly assume that there is a relationship between the true, three-dimensional velocity fields,  $v_i(x, y, z)$ , and the DA velocity fields,  $\bar{v}_i(x, y)$ . The lid and bottom shear stresses in equation 5 are obtained from this relationship.

First consider laminar flow. For fully-developed laminar flow between parallel plates the velocity profile can be written

$$v_x(x, y, z) = 6\bar{v}_x(x, y) \left[ \left(\frac{z}{h}\right)^2 - \left(\frac{z}{h}\right) \right] \quad (7)$$

where  $z$  is the direction normal to the plates,  $h$  is the plate spacing, and  $\bar{v}_x$  is the average velocity. Given this profile the wall shear stress terms are

$$(\tau_{z,x})_\ell = \frac{6\mu\bar{v}_x}{h} \quad (\tau_{z,x})_b = -\frac{6\mu\bar{v}_x}{h} \quad (8)$$

When the laminar flow equations are being solved, equations 8 are substituted into equation 5.

When the flow is turbulent the velocity profile for fully-developed turbulent flow in a parallel plate channel is used to specify the wall shear stress. In the DA model only the wall shear stress as a function of local mean (depth-averaged) velocity is needed. The wall shear stress is computed from the friction factor

$$f \equiv \frac{8\tau_w}{\rho\bar{u}^2} \quad (9)$$

where  $\bar{u}$  is the magnitude of the local DA velocity vector, i.e.,

$$\bar{u} = \sqrt{\bar{v}_x^2 + \bar{v}_y^2} \quad (10)$$

For a given flow the numerical value of  $f$  is computed from Prandtl's semi-empirical formula (Cebeci & Bradshaw, 1984)

$$\frac{1}{\sqrt{f}} = 0.87 \ln \left( Re \sqrt{f} \right) - 0.41 \quad (11)$$

where  $Re$  is the Reynolds number based on hydraulic diameter of the duct. We assume that for any one run of the DA model the value of  $f$  is constant, but that the local wall friction varies with  $\bar{u}$  according to equation 9. Thus, increases in local velocity correspond to local increases in the wall shear stress.

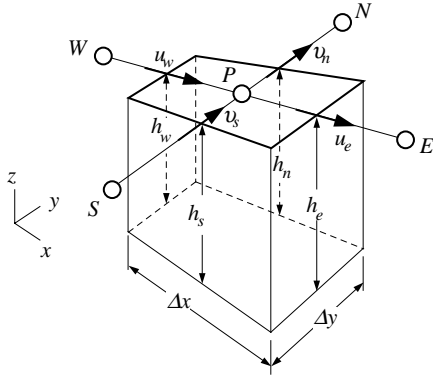


Figure 2: Control volume used to obtain the discrete forms of the depth-averaged momentum and continuity equations.

### Numerical Implementation

The DA model is implemented in a computer code based on the control-volume finite-difference formulation. The steady forms of equations 4 and 5 are integrated over the control volume shown in Figure 2. Note that the  $z$ -direction dimension of the control volume is the layer thickness,  $h$ .

The gap profile  $h(x, y)$  is specified at each computational node and is assumed to be uniform over each control volume. Thus, whenever there is a change in gap height, there is a discontinuous change in  $h$  at the boundary between adjacent control volumes. We chose discontinuous gap height variation instead of the continuous gap variation as suggested by Figure 1 because the geometry of PCBs involves step changes in component height. Step changes in gap height means that the area of adjacent control volume faces is not equal. In computing the flow of conserved variables from one control volume to the next the flux is continuous and the flow area is the minimum of the flow area of the two adjacent control volume faces. In this way we maintain the conservative properties of the control-volume finite-difference formulation.

Coupling between the momentum and continuity equations in the DA model is achieved with the SIMPLER algorithm (Patankar, 1980). Additional details on implementing the DA model are discussed by Rodi et al. (1981) and Choudhury (1986).

### The Pressure Field

The DA pressure field satisfies the discrete form of the DA momentum and continuity equations, cf. equations 4 and 5. The discontinuous changes in fluid layer thickness result in discontinuous velocity and pressure fields as demonstrated in the following example

Consider the two-dimensional flow situation depicted in Figure 3. A single rectangular rib extends across the entire width of a parallel plate channel. The rib height is chosen to

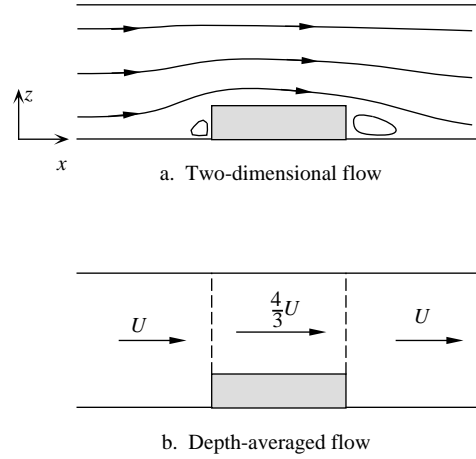


Figure 3: Flow in a parallel plate channel having a single rectangular rib attached to the bottom plate. The upper figure depicts the actual, two-dimensional flow. The lower figure shows the depth-averaged flow field when the rib height is equal to one fourth of the channel height.

be one fourth of the channel height, though the actual size of the rib is unimportant for the current analysis. The upper figure is a qualitative representation of the two-dimensional flow pattern. The lower figure shows the corresponding DA flow field. The variation of the DA velocity can be obtained directly from the continuity equation, i.e.

$$\frac{\partial}{\partial x} (\bar{v}_x h) = 0 \Rightarrow \bar{v}_{x,1} h_1 = \bar{v}_{x,2} h_2 \quad (12)$$

where subscripts 1 and 2 indicate any two stations along the channel. Equation 12 shows that step changes in the fluid layer thickness require step changes in the DA velocity.

The DA pressure is also discontinuous at these jumps in layer thickness. It is possible to directly compute the pressure distribution for the one-dimensional pathological case depicted in Figure 3. Results of such calculations for  $Re_H = 2HU/\nu = 100$  are shown in Figure 4. The two curves are for channel to rib height ratios of 1/2 and 1/4 respectively. The pressure is made dimensionless with the dynamic head,  $\frac{1}{2}\rho U^2$  and the inlet pressure for both cases is set equal to zero. The spike in the pressure at the leading edge of the rib also occurs in the multidimensional version of the DA flow field as shown by results in (Recktenwald, 1995).

### Energy Equation

The three-dimensional energy equation is

$$\frac{\partial}{\partial x_i} (\rho v_i T) = \frac{\partial}{\partial x_i} \left[ \left( \frac{k}{c_p} + \rho \varepsilon_H \right) \frac{\partial T}{\partial x_i} \right] + \frac{S_T}{c_p} \quad (13)$$

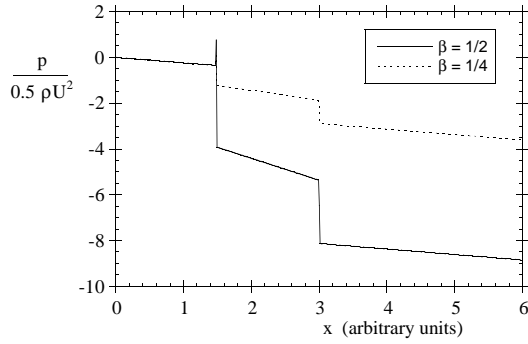


Figure 4: Depth-averaged pressure for one-dimensional flow in a parallel plate channel having a single rectangular rib attached to the bottom plate. The rib extends from  $x = 1.5$  to  $x = 3$ . The two curves are for rib to channel height spacing ratios of  $1/2$  and  $1/4$ , respectively. The Reynolds number based on plate spacing is 100 for both curves.

where  $v_i$  are the local, three-dimensional velocity components,  $\rho$  and  $c_p$  are the density and specific heat of the fluid,  $k$  is the thermal conductivity of the fluid or solid (depending on position in the domain),  $\varepsilon_H$  is the eddy diffusivity for energy transport, and  $S_T$  is the volumetric heat generation rate resulting from the dissipation of electrical power. To solve this equation, the DA velocity field obtained by solving equations 4 and 5 must be expanded to occupy the entire fluid layer.

The energy equation needs a three-dimensional flow field, but the DA model contains no information about the  $v_z$  velocity component. In addition, use of the DA flow field in the 3D model requires the introduction of assumptions about the shape of the  $v_x$  and  $v_y$  velocity profiles in the  $z$  direction, and the extent of the flow in the  $z$  direction.

In an earlier paper (Ma & Recktenwald, 1993) extensive quantitative comparisons were made between predictions of the 3D energy equation model and experiments. The accuracy of the predictions was found to depend on the assumed shape of the velocity profile (uniform or fully-developed). For some data sets the uniform profile gave better results and for other data sets the fully-developed profile gave better results. The option of using either type of profile is retained in the 3D energy equation code.

When the fully-developed profile is used the  $z$  variations of the  $v_x$  and  $v_y$  components are obtained from the same profile assumption that determines the top and bottom shear stresses appearing in equation 5. When the uniform profile is used the velocity components at all  $z$  positions are set equal to their values obtained from the DA model at a given point in the  $x$ - $y$  plane. In either case the profiles are specified such that mass is conserved for each control volume and for the domain as a whole.

Step changes in channel height, as in Figure 3, cause problems in interpreting the DA flow field in the energy equation model. The velocity field in equation 13 is three-dimensional. The  $z$ -direction variation of  $v_x$  is obtained from the profile assumption used to compute the wall shear stress in the DA model. This still leaves a question of how to account for the vertical velocity component necessary to maintain mass conservation immediately upstream and downstream of step changes in channel height.

After some experimentation the following procedure was chosen for assigning the velocity field in the 3D model. For any circuit board, define the fluid gap,  $h_g$  as the distance from the top of the tallest electronic component to the lid of the fluid layer. This fluid gap is depicted in Figure 5. We then arbitrarily assert that all the flow is confined to this gap. This is at least qualitatively consistent with experimental and numerical results obtained by other researchers, see e.g. Garimella and Eibeck (1991) and Kim and Anand (1995). The assumption of a uniform gap for the flow is used only in the 3D model. The DA model includes the changes in bottom surface topology, and the velocity field satisfying equations 4 and 5 reflect the blockage effects of electronic devices and other obstacles. Because the flow in the 3D model is confined to the gap, the DA velocity components must be scaled so that the flow rate is the same in both models. The is achieved with the following simple calculations

$$\tilde{v}_x = \bar{v}_x \frac{h}{h_g} \quad \tilde{v}_y = \bar{v}_y \frac{h}{h_g} \quad (14)$$

where  $\tilde{v}_x$  and  $\tilde{v}_y$  are the scaled, DA velocity components exported to the 3D model.

This model has the following consequences. There are no  $z$ -direction velocity components in the 3D flow field. The fluid velocity is zero at all points below the gap. The accuracy of this flow model will degrade as the variation in component heights on the circuit board increase. Because the flow is confined to the gap, the fluid velocities in the gap will be somewhat higher than they would be in a real circuit board. One might therefore expect that the model will overpredict the heat transfer rate from the top of the components. On the other hand, the model will underpredict the heat transfer rate from the sides of the components.

The flow model just described is not likely to give highly accurate results for heat transfer from isolated components. For a densely populated circuit board, however, the flow will predominantly occur in the space above the components, and the DA flow model should be more applicable. It is for such densely populated circuit boards that thermal management is most critical, and the models described here should be useful in these situations.

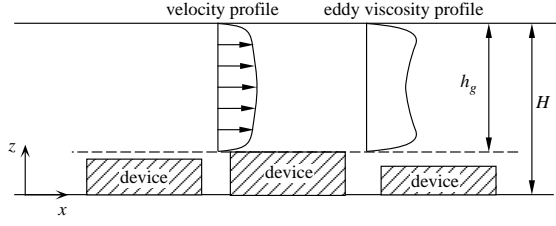


Figure 5: Two dimensional (elevation view) representation of the velocity profile used in the PCBCAT model. The shaded boxes labeled “device” are electronic components attached to the bottom surface of the domain.

### Fully-Developed Flow Profiles

Use of fully-developed profiles in the 3D model involves calculating the local,  $z$ -direction variation of the velocity components as function of the local, scaled, DA velocity values. For laminar flow, the  $z$  variation of the  $v_x(x, y, z)$  and  $v_y(x, y, z)$  velocity components are computed from equation 7 where the  $\tilde{v}_j$  from equation 14 are used in place of  $\tilde{v}_j$ , and  $h_g$  is used in place of  $h$ .

For turbulent flow the fully developed turbulent profile is evaluated with the procedure recommended by Cebeci and Bradshaw (1984). This is different from earlier work (Ma & Recktenwald, 1993), where we developed our own procedure for assigning the velocity and eddy viscosity profiles. The fully-developed turbulent profile is applied to the local, DA velocity vector, not to the separate DA velocity components. Let  $\bar{u}$  be the magnitude of the local, DA velocity as defined in equation 10. Then  $u(z)$  is the local velocity profile with average velocity equal to  $\bar{u}$ . Once  $u(z)$  is known the components  $v_x(x, y, z)$  and  $v_y(x, y, z)$  are computed from

$$v_x(x, y, z) = u(z) \cos \theta \quad v_y(x, y, z) = u(z) \sin \theta \quad (15)$$

where

$$\tan \theta \equiv \frac{\tilde{v}_y(x, y)}{\tilde{v}_x(x, y)} \quad (16)$$

As recommended by Cebeci and Bradshaw (1984), the  $u(z)$  profile is obtained by numerically integrating

$$u^+ = \int_0^{y^+} \frac{2}{1 + \sqrt{1 + 4(L^+)^2}} dy^+ \quad (17)$$

where  $L^+$  is a dimensionless length scale including a van Driest damping term,

$$L^+ = l^+ \left[ 1 - \exp\left(-\frac{y^+}{A^+}\right) \right] \quad (18)$$

$l^+$  is a length scale adapted from Nikuradse’s mixing length formula,

$$l^+ = \quad (19)$$

$$\frac{u_\tau z_m}{\nu} \left[ 0.14 - 0.08 \left( 1 - \frac{z}{z_m} \right)^2 - 0.06 \left( 1 - \frac{z}{z_m} \right)^4 \right]$$

and  $z_m$  is the midpoint of the fluid layer. In the preceding equations the velocity scale is the friction velocity  $u_\tau \equiv \sqrt{\tau_w / \rho}$  where  $\tau_w$  is evaluated from equation 9.

Equation 17 is integrated for each column of control volumes in the  $x$ - $y$  plane. The result is a profile,  $u(z)$  of the velocity magnitude based on the magnitude of the DA velocity at a given point  $(x, y)$  in the plane.

### Turbulence Model

The effect of the Reynolds stresses in enhancing the apparent diffusion of momentum and heat is simulated with a simple eddy viscosity model.

In the 3D energy equation model the eddy viscosity profile is evaluated with the procedure recommended by Cebeci and Bradshaw (1984). At each  $x$ - $y$  position along the duct, the  $z$ -direction variation of the eddy viscosity profile is calculated from

$$\varepsilon_m = \nu \left\{ l^+ \left[ 1 - \exp\left(-\frac{y^+}{A^+}\right) \right] \right\}^2 \frac{du^+}{dy^+} \quad (20)$$

where  $du^+/dy^+$  is the integrand of equation 17. The eddy diffusivity for thermal energy transport is obtained by assuming that the turbulent Prandtl number equals one, i.e.,  $\varepsilon_H = \varepsilon_m / Pr_t$  with  $Pr_t = 1$ .

In the DA model the effective viscosity is taken to be  $\mu_e = \mu + \rho \varepsilon_{m,o}$  where  $\varepsilon_{m,o}$  is the value of  $\varepsilon_m$  at the midpoint of the duct as calculated from equation 20. A single value of  $\varepsilon_{m,o}$  is used throughout the DA calculation domain.

### Numerical Implementation

The 3D energy equation model is implemented in a computer code based on the control-volume finite-difference formulation. The discrete form of the 3D energy equation is obtained from equation 13 using standard practices for three-dimensional equations. Refer to Patankar (1980) for details.

The convection modeling scheme in both the DA and 3D energy equation models is first order upwinding. This is widely known to lead to artificial smearing of gradients. Given the many other approximations built into the models we felt that the first order upwinding provides acceptable accuracy for the current implementation.

### Object-Based Data Structures

Specification of the physical problem and control of the numerical solution is achieved via commands to a preprocessor, which is described in a companion paper (Recktenwald, 1995). The preprocessor separates the user from in-

ternal minutiae of the analysis codes, such as the node numbering or the number of degrees of freedom to specify at a boundary. Given input from the user, the preprocessor builds its internal description of the problem by assembling lists of geometric objects. These objects are either probes, patches, or blocks. (Higher level objects, e.g., electronic devices, are under development, but have not been completely implemented as of this writing.) The analysis codes and preprocessor are written in C, which allows for the explicit creation of the probe, patch, block, etc. data types. The object data types are used throughout the analysis codes except for the solution of the linearized equations.

The CFD analysis is performed on a structured Cartesian grid having control volume faces that are aligned with the edges of the objects in the domain. The user specifies tolerances on the largest acceptable size of the computational cells and the analysis codes separately construct their own grids. After the analysis grid is created, the analysis codes use the preprocessor-defined objects to specify material properties, boundary conditions, and ultimately, to extract data for presentation to the user as output.

### Solution Algorithm

The discrete equations in both DA and 3D energy equation models are solved by line relaxation augmented with one-dimensional block correction (Settari & Aziz, 1973; Hutchinson & Raithby, 1986). Solution of the discrete energy equation is complicated by the large differences in thermal conductivity for the materials occurring in electronic cooling applications. Aluminum, for example, has a thermal conductivity that is approximately 7000 times larger than the thermal conductivity of air. This leads to large variations in the magnitudes for the coefficients of the discrete equations, which in turn leads to large condition numbers for the linear system of equations. Relaxation-based iterative solvers converge slowly when the condition number of the linear system is large. We have found that a simple, explicit block correction scheme (Kelkar, 1989) significantly enhances convergence when used in addition to one dimensional block correction and line relaxation. The explicit block correction scheme involves making additive corrections to regions of the domain with equal thermal conductivity. This is easily implemented with the object-based data-structures described in the preceding section.

### Future Work

Several extensions and improvements to the analysis codes can be envisioned. These can be categorized into (1) extensions to the modeling capabilities, (2) improvements in computational efficiency, and (3) development of entirely new modeling strategies.

In extending the modeling capabilities of the current

codes the first task is to complete the "device" object that will be used to model electronic components. Another obvious improvement is to extend the analysis solution of the energy equation down into the circuit board itself. These improvements involve straightforward modifications of the current codes.

Current execution times are reasonable on workstation class computers. The primary reason for the efficiency of these methods is the mathematical simplifications built into the DA model. For very complex models, further reduction in execution times may be achieved by using more sophisticated solution algorithms, e.g., multigrid, for the DA equations and preconditioned Krylov methods for solution of the energy equation.

Perhaps the most significant enhancement to the current codes will come through the development of new modeling strategies. We have obtained interesting preliminary results involving a two-and-one-half dimensional (2.5 D) model as a replacement for the DA model. Should this approach prove to be successful it will remove the need to use fully-developed flow models for the bottom and lid shear stress, and for the  $z$ -direction variation of the velocity fields in the 3D energy equation model. The 2.5 D flow model also eliminates the spurious spikes in the pressure that occur for the DA velocity field. Turbulence modeling is another area in which improvements could have a significant impact on the accuracy of the current codes. Finally, developing efficient models for mixed convection flows would greatly expand the applicability of these codes.

### Conclusion

This paper summarizes a numerical modeling strategy designed specifically for convectively cooled printed circuit boards. The model is based on CFD, but several simplifying assumptions have been introduced to make the analysis more computationally efficient.

### Acknowledgments

This research was supported by a grant from Intel Corporation. Dr. Muralidhar Tirumala of the Intel Architectural Development Laboratory supervised the development of these codes and gave technical advice on modeling electronic components.

### REFERENCES

- Agonafer, D., & Moffatt, D.F. 1990. Numerical modeling of forced convection heat transfer for modules mounted on circuit boards. *Journal of Electronic Packaging*, **112**(4), 333–337.

- Anderson, A. M. 1993. A comparison of computational and experimental results for flow and heat transfer from an array of heated blocks. *Pages 583–591 of: Engel, Peter A., & Chen, William T. (eds), Advances in Electronic Packaging 1993*, vol. EEP-Vol. 4–2. ASME.
- Anderson, A. M. 1994. Decoupling convective and conductive heat transfer using the adiabatic heat transfer coefficient. *Journal of Electronic Packaging*, **116**(4), 310–316.
- Cebeci, Tuncer, & Bradshaw, Peter. 1984. *Physical and Computational Aspects of Convective Heat Transfer*. New York: Springer-Verlag.
- Chen, K.S., & Chang, Y.R. 1987. Thermal-network simulation of printed circuit boards within a naturally ventilated cabinet. *In: Bartoszek, J., Furkay, S., Oktay, S., & Simons, R. (eds), Temperature/Fluid Measurements in Electronic Equipment: HTD-Vol. 89*, vol. HTD-Vol. 89. New York: ASME.
- Choudhury, Dipankar. 1986. *A Quasi-three-dimensional calculation procedure for the prediction of flow and heat transfer in heat exchanger passages*. Ph.D. thesis, University of Minnesota.
- Currie, I.G. 1993. *Fundamental Mechanics of Fluids*. Second edn. New York: McGraw-Hill.
- Davalath, J., & Bayazitoglu, Y. 1987. Forced convection cooling across rectangular blocks. *Journal of Heat Transfer*, **109**, 321–328.
- De Mey, G., & Van Schoor, L. 1988. Thermal analysis of hybrid circuits with mounted components. *Hybrid Circuits*, **15**(Jan), 28–32.
- Ellison, Gordon N. 1989. *Thermal Computations for Electronic Equipment*. Malabar, FL: Robert Krieger Publishing Co.
- Garimella, S.V., & Eibeck, P.A. 1991. Fluid dynamic characteristics of the flow over an array of large roughness elements. *Journal of Electronic Packaging*, **113**(4), 367–373.
- Hardisty, H., & Abboud, J. 1990. Thermal analysis of microelectronic systems using finite element modeling. *Pages 999–1013 of: Bergles, A.E. (ed), Heat Transfer in Electronic and Microelectronic Equipment*. New York: Hemisphere.
- Hutchinson, B.R., & Raithby, G.D. 1986. A multigrid method based on the additive correction strategy. *Numerical Heat Transfer*, **9**, 511–537.
- Incropera, F.P., Kerby, J.S., Moffatt, D.F., & Ramadhyani, S. 1986. Convection heat transfer from discrete heat sources in a rectangular channel. *International Journal of Heat and Mass Transfer*, **29**(7), 1051–1058.
- Kelkar, Kanchan M. 1989. *An efficient iterative solution method for the numerical prediction of heat transfer in problems involving large differences in thermal conductivity*. Tech. rept. 89-1684. AIAA.
- Kim, S.H., & Anand, N.K. 1995. Laminar heat transfer between a series of parallel plates with surface-mounted discrete heat sources. *Journal of Electronic Packaging*, **117**(Mar), 52–62.
- Ma, Yidong, & Recktenwald, Gerald W. 1993. Simplified Simulation of Convective Heat Transfer From an Array of Heated Blocks in a Rectangular Channel. *Pages 609–618 of: Engel, Peter A., & Chen, William T. (eds), Advances in Electronic Packaging 1993*, vol. EEP-Vol. 4–2. ASME.
- Moffat, R.J., & Ortega, A. 1988. Direct air-cooling of electronic components. *Pages 129–282 of: Bar-Cohen, A., & Kraus, A.D. (eds), Advances in Thermal Modeling of Electronic Components and Systems*, vol. 1. New York: Hemisphere.
- Patankar, S.V. 1980. *Numerical Heat Transfer and Fluid Flow*. Washington D.C.: Hemisphere.
- Recktenwald, Gerald W. 1995. Using the PCBCAT to model convective heat transfer from electronic devices on printed circuit boards. *In: Proceedings of 1995 International Mechanical Engineering Congress and Exposition*. San Francisco, CA: ASME.
- Rodi, W., Pavlovic, R.N., & Srivatsa, S.K. 1981. Prediction of flow and pollutant spreading in rivers. *Pages 63–111 of: Fischer, H.B. (ed), Transport Models for Inland and Coastal Waters*. New York: Academic Press.
- Settari, A., & Aziz, K. 1973. A generalization of the additive correction method for iterative solution of matrix equations. *SIAM Journal of Numerical Analysis*, **10**, 506–521.
- Zebib, A., & Wo, Y.K. 1989. A two-dimensional conjugate heat transfer model for forced air cooling of an electronic device. *Journal of Electronic Packaging*, **111**(Mar), 41–45.